



HAL
open science

Multivalent DNA recognition by self-assembled clusters: deciphering structural effects by fragments screening and evaluation as siRNA vectors

Eline Bartolami, Yannick Bessin, Nadir Bettache, Magali Gary-Bobo, Marcel Garcia, Pascal Dumy, Sébastien Ulrich

► To cite this version:

Eline Bartolami, Yannick Bessin, Nadir Bettache, Magali Gary-Bobo, Marcel Garcia, et al.. Multivalent DNA recognition by self-assembled clusters: deciphering structural effects by fragments screening and evaluation as siRNA vectors. *Organic & Biomolecular Chemistry*, 2015, 13 (36), pp.9427 - 9438. 10.1039/c5ob01404b . hal-03116768

HAL Id: hal-03116768

<https://hal.science/hal-03116768>

Submitted on 29 Sep 2021

HAL is a multi-disciplinary open access archive for the deposit and dissemination of scientific research documents, whether they are published or not. The documents may come from teaching and research institutions in France or abroad, or from public or private research centers.

L'archive ouverte pluridisciplinaire **HAL**, est destinée au dépôt et à la diffusion de documents scientifiques de niveau recherche, publiés ou non, émanant des établissements d'enseignement et de recherche français ou étrangers, des laboratoires publics ou privés.

Multivalent DNA recognition by self-assembled clusters: deciphering structural effects by fragments screening and evaluation as siRNA vectors

Received 00th January 20xx,
Accepted 00th January 20xx

DOI: 10.1039/x0xx00000x

www.rsc.org/

Eline Bartolami, Yannick Bessin, Nadir Bettache,* Magali Gary-Bobo, Marcel Garcia, Pascal Dumy and Sébastien Ulrich*

The identification of low-molecular-weight clusters that effectively complex oligonucleotides of therapeutic interest is of great importance for applications in gene delivery. We recently reported the use of self-assembly processes based on chemoselective ligation in order to generate biomolecular clusters for the multivalent recognition of DNA. Herein, we exploit the modularity of this methodology to perform a one-pot fragments screening of scaffolds and binding groups. Structural parameters affecting DNA binding were observed and hits have been identified by fluorescence displacement and gel electrophoresis assays. Finally, we evaluated the potential of these systems for siRNA transfection. One biomolecular cluster was found to effectively complex and transport a 21-mer siRNA inside MCF7 human breast cancer cells, resulting in a significant knockdown of the target gene.

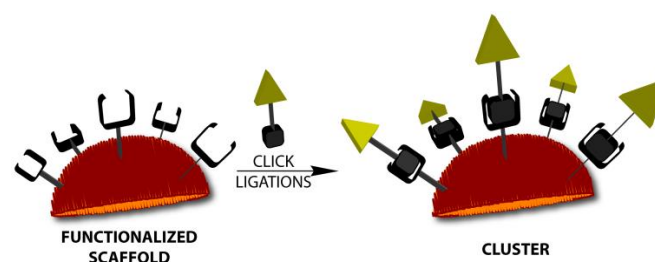
Introduction

Challenges in gene therapy. The prospect of treating the genetic root of diseases is a fascinating perspective of modern biotechnologies. Towards this goal, synthetic oligonucleotides represent therapeutic agents that can serve in antisense¹ and silencing technologies.² However, the effective and safe intracellular delivery of synthetic oligonucleotides remains a tremendous challenge. Oligonucleotides are negatively-charged biomolecules that are relatively unstable in biological medium – they undergo enzymatic degradation by nucleases – and cannot pass cell membranes due to electrostatic repulsion. Thus, the success of oligonucleotide-based therapeutics depends greatly on the development of effective vectors. The serious immunogenic effects displayed by viral vectors³ call for an alternative bottom-up chemical approach. The design of synthetic systems that effectively complex and transport oligonucleotides is therefore a topic of great importance.⁴

Synthetic macromolecular vectors. Cationic polymers⁵ and dendrimers⁶ have been extensively studied for the complexation and transport of oligonucleotides. In this case, the repetitions, within a single chain or compound, of multiple

binding units that promote complex formation with oligonucleotides exert a multivalent⁷ binding. However, the high molecular weight of these macromolecules is an issue and toxic side-effects have been observed due to their accumulation in biological tissues.⁸ A current approach for lifting these limitations focus on the generation of low-molecular-weight vectors that may be degradable and/or stimuli-responsive.^{9, 10}

Multivalent DNA recognition by low-molecular-weight clusters. The multifunctionalization strategy (Scheme 1), whereby a scaffold is functionalized with multiple copies of a binding group through click-type reactions, has been recently exploited for generating low-molecular-weight cationic clusters that effectively complex oligonucleotides despite their limited valency with respect to polymers.



Scheme 1 Schematic representation of the principle of cluster formation by multiple click ligations of a binding group (yellow triangle) onto a functionalized scaffold.

Different examples of low-molecular-weight clusters based on a variety of scaffolds (calixarene,^{11, 12} fullerene,¹³ pillar[5]arene,¹⁴ cyclodextrines,¹⁵ and dendrimers¹⁶) and ligands (ammonium, guanidinium) have thus been reported.

Institut des Biomolécules Max Mousseron (IBMM), UMR 5247, CNRS, Université Montpellier, ENSCM, Ecole Nationale Supérieure de Chimie de Montpellier, 8 Rue de l'École Normale, 34296 Montpellier cedex 5, France
E-mail: nadir.bettache@univ-montp2.fr; Sebastien.Ulrich@enscm.fr.

† Electronic Supplementary Information (ESI) available: [details of any supplementary information available should be included here]. See DOI: 10.1039/x0xx00000x

These systems represent promising alternatives to macromolecular vectors, provided their structures are finely tuned in order to optimize the multivalent binding to oligonucleotides.¹⁷ Effective screening methods are therefore needed for facilitating the identification of potent oligonucleotide-binding clusters.

We recently reported the generation of tetravalent biomolecular clusters based on cyclic peptide scaffolds for the multivalent recognition of DNA.¹⁸ In comparison with the most popular organic scaffolds, the use of biomolecules such as peptides as scaffolds is of interest in terms of biocompatibility. The selected bottom-up methodology rests upon the multifunctionalization of the cyclic peptide scaffold through acylhydrazone ligations. This type of ligation operates in mild aqueous conditions and can tolerate the presence of a complex biomolecular target such as DNA. Its chemoselectivity thus enables tethering in one-pot unprotected binding groups onto the scaffold. It is therefore a robust tool for programming the assembly of multiple fragments into a bioactive cluster. It has for instance been recently used by the Matile group for generating amphiphiles.¹⁹ The modularity of this fragment-assembly process of cluster formation through acylhydrazone ligations should enable the rapid screening of scaffolds and binding groups which, in turn, would help develop a better understanding of the molecular factors that determine the DNA-binding ability of these clusters. We report herein the results of a screening of different scaffolds and binding groups that are assembled together in a combinatorial fashion. The DNA-binding ability was directly analysed by a fluorescence-displacement assay and cross-checked by gel electrophoresis. Finally, the best hits were evaluated on cell culture as potential siRNA vectors.

Results and discussion

Design and synthesis of building blocks.

The clusters are formed by tethering, through acylhydrazone ligations, hydrazone binding groups onto functionalized scaffolds featuring reactive aldehyde moieties (Scheme 1). The selected functionalized scaffolds bear a varying number (functionality = 1-4) of reactive aldehyde groups (compounds **A**, Fig. 1). We selected different commercially-available compounds along with two synthetic – linear and cyclic – peptides. Thus, these scaffolds feature different (bio)molecular structures and valency. The hydrazone partners are derivatives of amino acids and tripeptides bearing a hydrazone group at their C-terminus. They feature different types of side groups (neutral, hydrophobic, anionic, cationic), different stereochemistry, and different valency (compounds **Hyd**, Fig. 1).

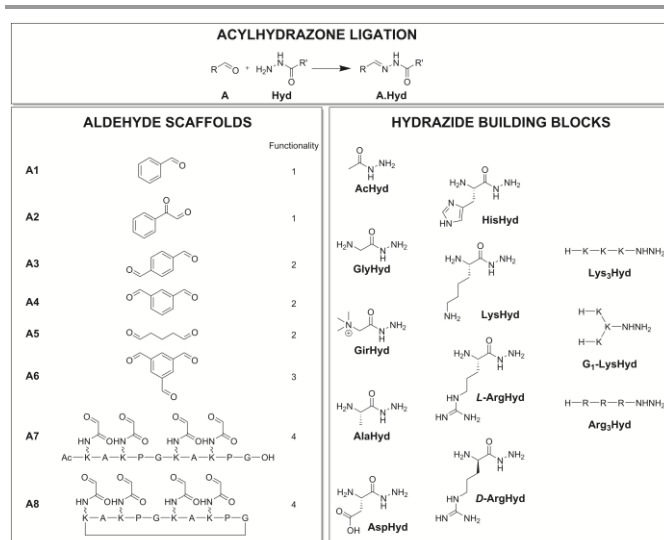


Fig. 1 Structure of aldehyde and hydrazone building blocks that are assembled through the acylhydrazone ligation.

The preparation of the linear peptide **A7** was adapted from the synthesis of the cyclic peptide **A8**,¹⁸ and involved solid-phase peptide synthesis, acetylation of the N-terminal, cleavage and deprotection, and oxidative cleavage of serine side-chains to unmask the glyoxylic aldehydes.

The hydrazone partners were synthesized by a solid-phase approach using a Fmoc-protected hydrazine resin that can be readily prepared by reacting the 2-chlorotrityl chloride resin with Fmoc-hydrazide (Fig. 2).²⁰ The amino acid hydrazides were prepared manually by peptide coupling, deprotection and cleavage. The tripeptide hydrazides were assembled using solid-phase peptide synthesis. After cleavage in mild acidic conditions, the protected peptides were purified by reverse-phase HPLC, before being fully deprotected to afford the tripeptide hydrazides.

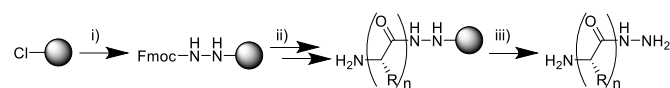


Fig. 2 Synthetic route for the preparation of amino acid and peptide hydrazides. i) Fmoc-hydrazide, DIEA; ii) a) deprotection: piperidine, b) peptide coupling: Fmoc-amino acid-OH, HATU, DIEA, c) deprotection: piperidine; iii) TFA/TIS/H₂O.

Self-assembly of clusters by acylhydrazone ligation.

The ligation reactions were carried out, as previously described, in aqueous buffer (100 mM AcONa, pH 5.0), with 1 mM of scaffolds **A** and 8 equivalents of hydrazide per scaffold. These conditions favour the formation of the bioconjugates **A.Hyd** of highest valency. To verify this and to demonstrate that the ligation proceeds equally well with respect to the different types of building blocks, we tested the cluster formation of all hydrazides with scaffold **A8** and of **AcHyd** with all scaffolds **A**. HPLC and mass spectrometry analyses confirm in all cases the formation of the corresponding clusters **A.Hyd** (see SI). These conditions are therefore suitable for the modular self-assembly of clusters from different scaffolds and binding groups. We therefore envisaged carrying out a one-pot

screening for rapidly identifying the structural determinants that favour multivalent DNA recognition.

Screening.

The ability of the different clusters to complex DNA was first assessed by a fluorescence displacement assay with ethidium bromide (EthBr) and calf thymus DNA (ctDNA). In this assay, a fluorescent emission decrease upon addition of a compound indicates its ability to complex DNA. This label-free assay is a simple method for establishing DNA binding affinity.²¹ It is also amenable to a high-throughput microplate format for enabling screening approaches,²² and it has already been used in this context for the determination of the DNA binding sequence selectivity of a ligand.²³ In this study, we selected this assay for comparing the DNA-binding ability of clusters formed from the combinatorial association of different fragments (scaffolds and binding groups).

In each well of a 96-well plate, we deposited one aldehyde scaffold **A** and one hydrazide building block (8 eq). After overnight mixing, acetate buffer (100 mM, pH 5.0) of low salinity (9.4 mM NaCl) followed by ctDNA and EthBr were subsequently added. DNA complexation by clusters results in a fluorescence decrease that occurs within hours. The results show strong differences in the fluorescence emission, which indicates strong differences in DNA-binding properties (Fig. 3).

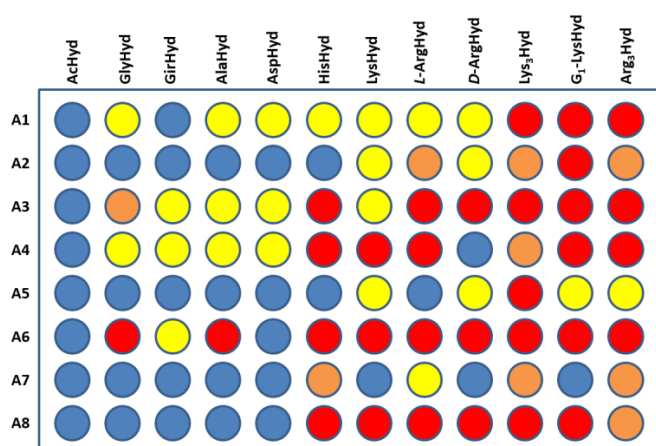


Fig. 3 Screening of a combinatorial array of aldehyde scaffolds **A** (left) and hydrazide binding groups (top) – assembled together by acylhydrazone ligations – by the ethidium bromide displacement assay with calf-thymus DNA target. Relative fluorescence emission ($\lambda = 590$ nm) decrease: 0-25% (●), 25-50% (●), 50-75% (●), 75-100% (●). Measurements performed 6 hours after the addition of the DNA target.

When looking at the differences between the different hydrazide binding groups, one can note that no DNA complexation occurs with **AcHyd**, regardless the nature of the scaffold it is assembled onto. In contrast, DNA complexation is detected with cationic binding groups. These results are in line with our previous observations that **A8.Ac** does not complex ctDNA while **A8.L-Arg** is an effective DNA-binding cluster,¹⁸ and thus validates this microplate format assay.

Effect of multivalency. These results suggest a multivalent effect since there are more hits with the tetravalent scaffold **A8** than with the monovalent **A1**. The comparison of these results with the DNA-binding ability of individual components

confirms that multivalency is a major factor that account for DNA-binding. Indeed, when tested alone by the EthBr assay, the individual aldehyde scaffolds **A** were found unable to complex ctDNA under these conditions (Fig. 4). Similarly, the individual hydrazide binding groups show no DNA complexation under these conditions, except for the tripeptides **Lys₃Hyd**, **G₁-LysHyd**, and **Arg₃Hyd** (Fig. 4).

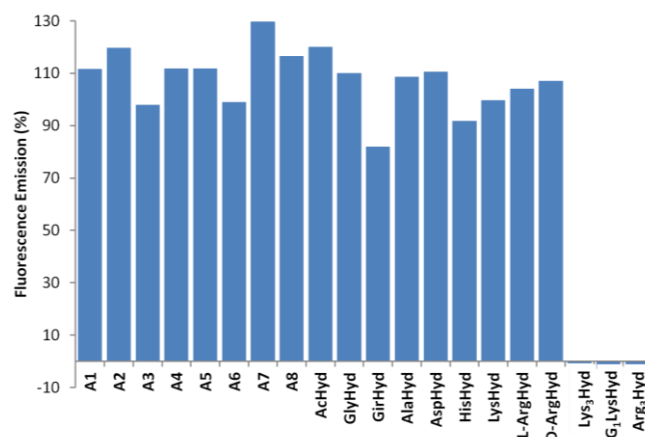


Fig. 4 DNA complexation by individual aldehyde scaffolds and hydrazide binding groups determined by EthBr assay.

Gel retardation assays confirm the role of multivalency and reveal the stoichiometry that is necessary for DNA binding – expressed by the N/P ratio of positive charges brought by the clusters per negative charges in DNA. For instance, no complexation was detected with **L-ArgHyd** in the range of N/P = 20-500 while the tetravalent cluster **A8.L-Arg** complexes plasmid DNA effectively at N/P \geq 20.¹⁸ Similarly, we found that the tripeptide **Arg₃Hyd** and the corresponding tetravalent cluster **A8.Arg₃** complexes DNA at N/P \geq 600 and N/P \geq 1, respectively (Fig. 5).

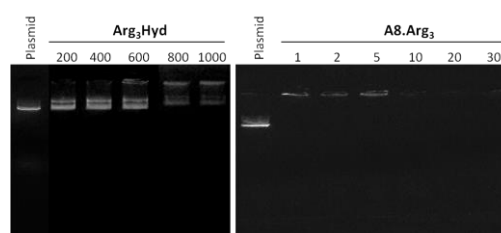


Fig. 5 Gel electrophoresis analysis showing the complexation of plasmid DNA by the tripeptide **Arg₃Hyd** (left) and the corresponding tetravalent cluster **A8.Arg₃** (right) at different N/P.

Effect of scaffolds. With the **L-ArgHyd** binding group, we previously found that, when it is assembled onto the tetravalent scaffold **A8**, the corresponding cluster **A8.L-Arg** is an effective DNA-binding agent.¹⁸ The results of the EthBr screening assay indicate that both the valency and the structure of the scaffolds have a strong impact on the DNA-binding ability of these clusters. Thus, divalent scaffolds **A3**, **A4** and tri- and tetra-valent scaffolds **A6**, **A8** yield DNA-binding clusters. The gel retardation assay confirms the importance of

scaffold structure but tends to indicate a weaker binding of the divalent clusters compared to the tri- and tetra-valent ones (Fig. 6).

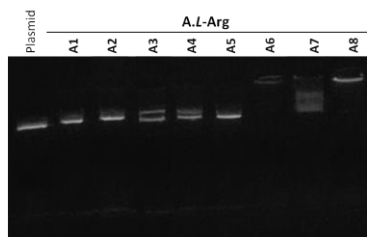


Fig. 6 Gel electrophoresis analysis showing the complexation of plasmid DNA by clusters made of different scaffolds **A** with hydrazide **L-ArgHyd**. Experiments carried out at $N/P=80$.

Similarly, with **Arg₃Hyd**, the gel retardation assay carried out at $N/P=1$ confirms the importance of the scaffold and reveals the superiority of the same scaffolds: **A3**, **A4**, **A6**, and **A8** (Fig. 7).

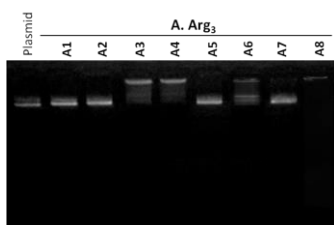


Fig. 7 Gel electrophoresis analysis showing the complexation of plasmid DNA by clusters made of different scaffolds **A** with hydrazide **Arg₃Hyd**. Experiments carried out at $N/P=1$.

Along these studies, we noticed a strong difference of DNA-binding ability between the clusters derived from the linear and cyclic scaffolds, respectively **A7** and **A8**. According to EthBr displacement assay, the cyclic cluster is more effective than the linear one for DNA complexation. The gel retardation assay confirms the superiority of the cyclic cluster over the linear one. Indeed, while the cyclic cluster bind effectively plasmid DNA at $N/P \geq 20$, the linear cluster is only effective at $N/P \geq 50$ (Fig. 8).

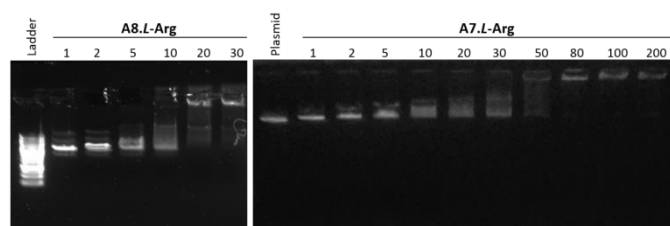


Fig. 8 Gel electrophoresis analyses showing the complexation of plasmid DNA by clusters **A8.L-Arg** (left) and **A7.L-Arg** (right) at different N/P .

While it remains unclear why the cyclic scaffold leads to a more effective DNA complexation compared to the linear one, this observation has been previously made with other cationic clusters.¹² In the present case, it is possible that the high pre-organization offered by the constraint cyclic peptide scaffolds **A8** is at the origin of this effect by increasing the local

concentration of positive charges, thereby minimizing the entropic penalty upon binding.

Effect of binding groups. The screening result shows that, while neutral (**AcHyd**) or anionic hydrazide (**AspHyd**) give no sign of DNA complexation when assembled on a scaffold, not all cationic hydrazide give rise to DNA complexation when assembled on a scaffold. For instance, the clusters featuring the Girard's reagent (**GirHyd**) form poor DNA-binding agents with most scaffolds even though it is positively charged. This indicates that, while electrostatic interactions may be important for DNA complexation, other interactions such as hydrogen bonds must be considered as well. Gel retardation assay confirms the general trend obtained by the EthBr screening and indicates that, with the scaffold **A8**, amino acids and tripeptides that contain lysine or arginine are the best binding groups (Fig. 9). A similar preference was observed with the scaffold **A6** (see SI).

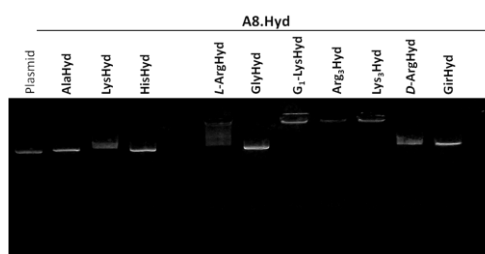


Fig. 9 Gel electrophoresis analysis showing the complexation of plasmid DNA by clusters made of scaffold **A8** with different hydrazides. Experiments carried out at $N/P=40$.

The absence of DNA complexation observed by gel electrophoresis with amino acids of low pKa (His, Lys) is in contrast with the EthBr assay but is most likely explained by pH effects since the former was carried out at pH 8.0 while the latter was carried out at pH 5.0.²⁴

The screening results also show that the amino acids bearing no positive charges on their side groups, such as **GlyHyd** and **AlaHyd**, do not yield potent DNA binders when assembled onto the tetravalent scaffold **A8**, thereby indicating that the presentation of α amino groups is not sufficient for promoting DNA binding. Nevertheless, when tested at $N/P=80$ by the EthBr assay (pH 5.0), DNA complexation with cluster **A8.Gly** can be detected. The comparison of DNA complexation properties with cluster **A8.L-Arg** shows that, while the latter does complex DNA effectively at low $N/P=2$ and high salinity (150 mM NaCl), the former only binds DNA at high $N/P=80$ and low salinity (9.4 mM NaCl) (Table 1).

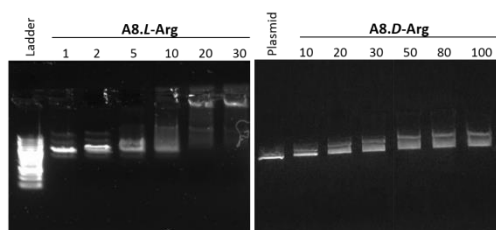
Table 1 ctDNA complexation, assessed by fluorescence displacement assay, by clusters **A8.L-Arg** and **A8.Gly** in different conditions.

Entry	Compounds	N/P ^[a]	[NaCl] (mM)	Fluorescence Emission (%) ^[b]
1	A8.L-Arg	80	9.4	2.6
2	A8.L-Arg	2	9.4	0
3	A8.L-Arg	80	150	25.3
4	A8.Gly	80	9.4	3.6
5	A8.Gly	2	9.4	100
6	A8.Gly	80	150	92.4

[a] N/P represents the ratio of positive charges (N) per phosphodiester (P);
 [b] measured after 20 hours.

Gel retardation assays (pH 8.0) support this conclusion by showing no DNA complexation with cluster **A8.Gly** in the range of N/P = 10-80 while cluster **A8.L-Arg** clearly complexes DNA at N/P \geq 20 (see SI).¹⁸

We were intrigued by the apparent differences in DNA-binding ability between clusters **A8.L-Arg** and **A8.D-Arg** (Fig. 9). A cross-analysis by gel electrophoresis at different N/P confirms that, indeed, the chirality of the binding group has a strong influence over the DNA-binding ability of the corresponding clusters (Fig. 10). With cluster **A8.D-Arg**, the gel retardation assay shows, in the range of N/P = 10-100, the appearance of a band slightly above the band of plasmid DNA. Compared to the results obtained with cluster **A8.L-Arg**, this suggests a weaker DNA complexation and most probably indicates different structures of the complexes with DNA. Again, this result suggests that long-range electrostatic interactions are not the sole responsible for the interactions between such cationic biomolecular clusters and DNA.

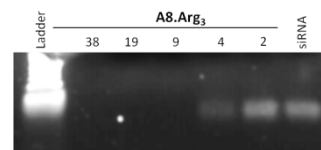
**Fig. 10** Gel electrophoresis analyses showing the complexation of plasmid DNA by clusters **A8.D-Arg** (right) compared to **A8.L-Arg** (left) at different N/P.

Overall, the fragments screening methodology enabled the rapid and successful identification of clusters that effectively bind DNA. The combination between the pre-organized scaffold **A8** and hydrazide binding groups featuring L-arginine(s) leads to the most effective complexation of DNA.

Biological evaluation.

The potential of clusters **A.Hyd** as siRNA vectors was then evaluated on a MCF7-luc cell line which is derived from MCF7 human breast cancer cells transfected by firefly luciferase gene. We first studied the cluster **A8.L-Arg**. Although dynamic light scattering (DLS) experiments confirm complex formation with siRNA and indicate a particle diameter of 148-190 nm at N/P=20, no significant evidence of cell penetration and

transfection efficacy were observed by, respectively, fluorescence imaging and cell luciferase assay (data not shown). We then turned our attention to the more effective cluster, **A8.Arg₃**. Gel retardation assay confirms complex formation with siRNA at N/P \geq 9 (Fig. 11).

**Fig. 11** Gel electrophoresis analyses showing the complexation of siRNA by cluster **A8.Arg₃** at different N/P.

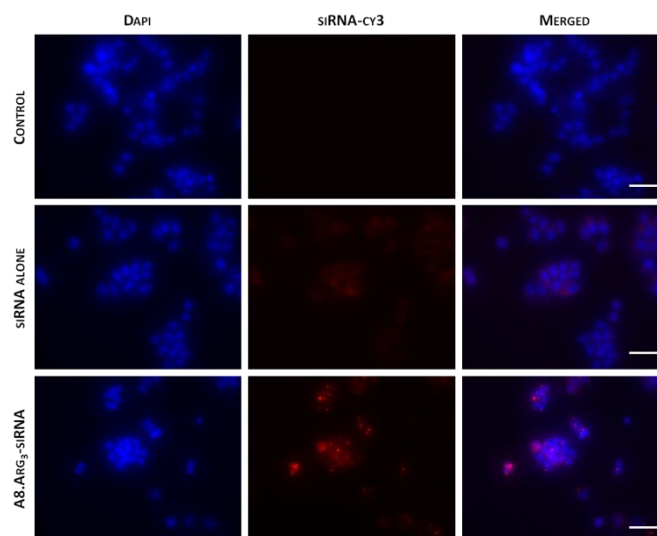
Similarly, DLS also shows complex formation with siRNA at N/P=9. The particles that are formed have diameter around 200 nm (PDI=0.1-0.2) and show good stability over time. In physiological salt concentration, the particles have a hydrodynamic diameter of 320 nm (PDI=0.17) (Table 2).

Table 2 Particle size characterization by dynamic light scattering of the complex formed between cluster **A8.Arg₃** and siRNA at N/P=9. Results are expressed as mean \pm standard deviation (n = 3).

	t_0	After 1 hour	After 1 hour (154 mM NaCl)
Z-average ^[a]	179.3 \pm 1.2	201.8 \pm 1.9	320.4 \pm 30.0
PDI ^[b]	0.143 \pm 0.005	0.154 \pm 0.009	0.122 \pm 0.008

[a] hydrodynamic diameter in nm; [b] polydispersity index

Then, the internalization of these particles by the cancer cells was analysed by fluorescent microscopy. Satisfyingly, the fluorescence imaging carried out with a Cy3-labeled non-coding siRNA shows that the cluster **A8.Arg₃** effectively transfects siRNA inside MCF7 cells (Fig. 12). This conclusion was confirmed on another breast cancer cell line, MDA-MB-231 (see SI).

**Fig. 12** Fluorescence imaging (magnification 40x) of MCF7 cells, alone (top), with Cy3-labeled non-coding siRNA (middle), and with the complex formed between cluster **A8.Arg₃** and Cy3-labeled non-coding siRNA at N/P=9 (bottom). The blue fluorescence

(left) indicates the nuclei (DAPI staining), and red fluorescence (middle) indicates the Cy3-labeled siRNA. Bars represent 50 μm .

The luciferase assay carried out with the 21-mer siRNA targeting the expression of luciferase further shows that the cluster **A8.Arg₃** acts as an effective vector to deliver siRNA inside cells at N/P=9. A dose-dependent silencing of the expression of luciferase was observed by fluorescence spectroscopy with increasing amounts of siRNA being transfected (Fig. 13). The cell viability was assessed by a MTT assay and shows no significant cell toxicity up to 0.5 μM of cluster **A8.Arg₃** (Fig. 13). These results show that there is a range of concentration (0.1-0.5 μM siRNA) where the cluster **A8.Arg₃** shows good transfection efficacy and no cellular toxicity.

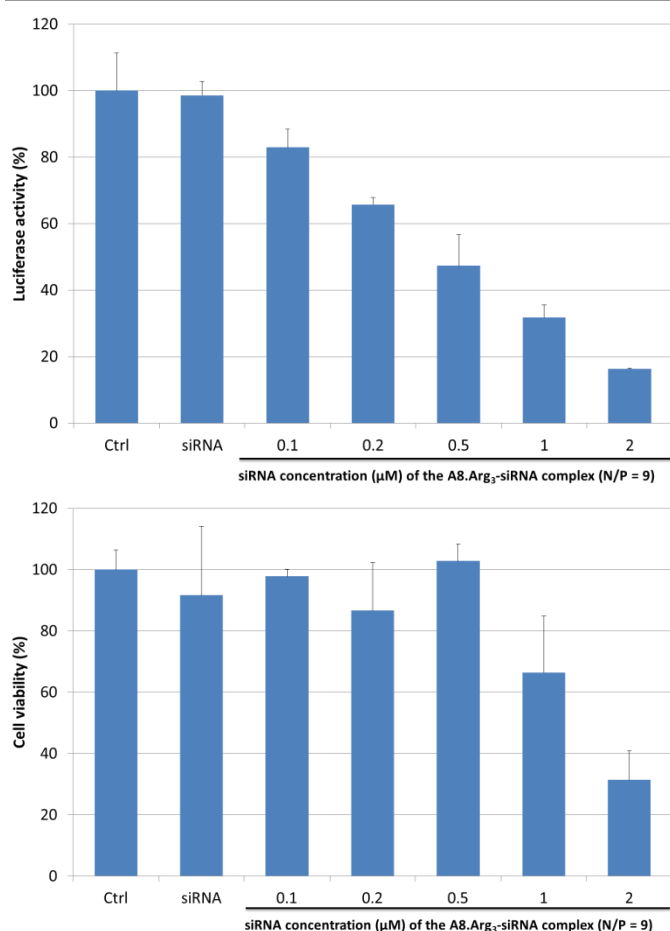


Fig. 13 Luciferase activity (top) and MTT cell viability (bottom) assays showing, respectively, the transfection of a 21-mer siRNA targeting the expression of luciferase inside MCF7-luc, and the viability of those cells. The experiments were carried out with increasing amounts of siRNA (0.1 to 2 μM) contained in the **A8.Arg₃**:siRNA complex (N/P=9). The results are expressed as mean \pm standard deviation ($n=3$).

Conclusions

We reported herein a rapid screening methodology for determining the DNA-binding ability of various clusters formed by acylhydrazone ligations. The results show that the structure of the scaffold has a profound impact on the multivalent recognition of DNA. Furthermore, the detailed role of binding

group structure and chirality has been evidenced. The potential of these clusters was then evaluated on cell culture and it was found that the most potent DNA-binding cluster also complexes, transports, and delivers effectively siRNA inside cells without displaying significant toxicity. The results pave the way towards the application of these biomolecular clusters as artificial vectors for the transport of oligonucleotides of therapeutic interest. Further chemical modifications of the hits identified herein will be studied in order to optimize the transfection efficacy by, for instance, attaching lipophilic tails.²⁵

Experimental

Materials and methods.

All solvents and chemical reagents were purchased from commercial suppliers and used without further purifications. Dry solvents were purchased in anhydrous quality from Fisher Scientific (Acros). For dichloromethane, amylene was the stabilizer. Calf-thymus DNA (ctDNA) was purchased from Sigma Aldrich.

NMR. NMR spectra were recorded on Bruker Avance 400 instruments and were referenced with respect to the residual solvent peak. Data are reported as follows: chemical shift (δ in ppm), multiplicity (s for singlet, d for doublet, t for triplet, q for quadruplet, m for multiplet, bs for broad signal), coupling constant (J in Hertz) and integration.

Mass spectrometry. MALDI-TOF and high resolution mass spectrometry analyses were carried out at the Laboratoire de Mesures Physiques, IBMM, Université de Montpellier, and were obtained, respectively, on an Ultraflex III and a Waters MicromassQ ToF mass spectrometer (positive mode).

HPLC. HPLC analyses were performed on a Waters HPLC 2695 (EC Nucleosil 300-5 C18, (125 x 3 mm) column, Macherey-Nagel) equipped with a Waters 996 DAD detector. The following linear gradients of solvent B (acetonitrile) into solvent A (100 mM triethylammonium acetate/acetonitrile 95/5) were used: 0 to 95% of solvent B in 45 min. Retention times (t_R) are given in minutes. Semi-preparative RP-HPLC was performed on a Waters 515 HPLC (VP Nucleodur HTec C18, 7 μm , (250 x 21) column, Macherey-Nagel) equipped with a Waters 2487 detector. Preparative HPLC was performed on a Waters Prep LC Controller HPLC (XSelect CSH Prep C18, 5 μm , (250 x 30 mm) column, Macherey-Nagel) equipped with a Waters 2489 detector.

SPPS. Solid-phase peptide synthesis (SPPS) was carried out on a Liberty, CEM[®] instrument equipped with microwave. The following conditions were used:

Solid support: 2-Chlorotrityl chloride resin.

Coupling conditions: Fmoc-AA-OH (3 eq.), HBTU (3 eq.), DIEA (5 eq.), DMF, 70°C for 5 min with microwave irradiation (0.25 mmol scale: 40 W, 0.1 mmol scale: 23 W). Double coupling (7 min) was used for arginine. In order to prevent diketopiperazine formation, the coupling of the amino acids next to Pro-Gly sequence was performed without heating or microwaves.

Deprotection conditions: Piperidine/DMF (2/8). 75°C/40 W for 30 sec, then 70°C/45 W for 3 min (twice).

Cleavage conditions: TFA/CH₂Cl₂ (1/99), then MeOH/Pyridine (8/2).

Fluorescence displacement assay. Ethidium Bromide displacement assays were carried out either in cuvettes (3 mL quartz cuvette for experiments with N/P=80, 0.5 mL quartz cuvette for experiments with N/P=2) on a Hitachi Fluorescence Spectrophotometer F-2500, or in COSTAR 96-Well plates on a SAFAS Monaco Xenius XML instrument. Excitation wavelength was set at 546 nm and emission was measured at 590 nm. The relative fluorescence emission decrease was calculated as follows:

$$\text{Fluorescence emission decrease (\%)} = \left(\frac{I_{\text{EthBr-DNA}} - I}{I_{\text{EthBr-DNA}} - I_{\text{EthBr}}} \right)$$

where $I_{\text{EthBr-DNA}}$ represents the fluorescence emission of the EthBr-ctDNA intercalation complex, I represents the measured fluorescence emission, and I_{EthBr} represents the fluorescence emission of EthBr in the absence of ctDNA.

The samples were prepared in the following buffers: i) sodium acetate (100 mM, pH 5.0), EDTA (10 μ M), NaCl (9.4 mM), or ii) Hepes buffer (100 mM, pH 7.2), EDTA (10 μ M), NaCl (9.4 mM), or iii) sodium acetate (100 mM, pH 5.0), EDTA (10 μ M), NaCl (150 mM).

Experiments in cuvette format were carried out as follows: Ethidium bromide was dissolved in the buffer to provide 42 μ M concentration and the fluorescence was measured. The appropriate amount of ctDNA was added from a stock solution in MilliQ H₂O to reach the desired N/P. The ligands were then added in microliters from 20-500 mM stock solutions in MilliQ H₂O to provide a final concentration of 1 mM in scaffold. The fluorescence measurement was recorded after shaking the solution a few seconds.

Experiments in 96-well plates were carried out as follows:

Scaffolds **A** (20 mM) and hydrazide building blocks **Hyd** (160 mM) were mixed in MilliQ H₂O, in each well, and left overnight at room temperature. Buffer, ctDNA, and EthBr were then added (final concentration in scaffold: 1 mM). The plates were shaken by orbital agitation (16 Hz, 120 sec), and the fluorescence emission was measured during 1 sec using a 1200 V voltage and a bandwidth of 6 nm for excitation and 10 nm for emission.

Gel electrophoresis. Gel retardation assays with plasmid DNA were performed using 100 ng of 5.7 kilobase pair expression vector pET-15b (Novagen), which were mixed with the appropriate amounts of ligand (in order to reach the desired N/P ratio) in 0.5X TAE (20 mM Tris-acetate/0.5 mM EDTA, pH 8.0) or 0.5X TBE (20 mM Tris-borate/0.5 mM EDTA, pH 8.0) buffer to obtain a final volume of 10 μ L. 2 μ L of Blue 6X loading dye (Fisher Scientific) was added, after which 12 μ L was run on a 0.7% agarose gel (50 V). DNA was visualized with SYBER Safe (Life Technologies) or SafeView PlusTM Nucleic Acid Stain (Euromedex). The reference for the gel is GeneRuler 1 kb DNA ladder (250 to 10000 bp) from Fischer Scientific. Gel retardation assays with siRNA were performed as follows: the cluster:siRNA complexes at a desired N/P were prepared in RNase free water with 300 ng of eGFP siRNA. Electrophoresis

was carried out on a 1 % wt/vol agarose gel in 1X TBE at 55 V for 1 h. The GelRed-stained siRNA was visualized on an ultraviolet transilluminator with a camera.

Dynamic light scattering. Particle size measurements were carried out on a Zetasizer Nano ZS (Malvern, United Kingdom) with transparent ZEN0040 disposable microcuvette cells (40 μ L) at 25°C. The cluster:siRNA complexes were prepared at a defined N/P ratio with a siRNA concentration of 1 μ M. Measurements were performed immediately after the complexes formation and after 1 h incubation. Then, NaCl solution was added at a final concentration of 154 mM and measurement was repeated.

Biological evaluation on cell culture. The MCF7-luc cell line derived from MCF7 human breast cancer cells by stable transfection of firefly luciferase gene (PCDNA 3.1 CMV-Luc-SVNeo) were generously provided by Dr P. Balaguer (ICM Montpellier, France). Selection of resistant clones was performed by geneticin addition at 1 mg.mL⁻¹ until experiments. Cells were grown in phenol red-free F12/Dulbecco's modified Eagle's medium (DMEM) supplemented with 10 % fetal calf serum (FCS). The cells were incubated at 37°C in a humidified atmosphere with 5% CO₂.

Cy3-labeled non-coding siRNA was purchased from Eurogentec (Serring, Belgium). The siRNA targeting sequence for luciferase (AACTTACGCTGAGTACTTCGA) was purchased from QIAGEN. The sense sequence is CUUACGCUGAGUACUUCGA and the antisense sequence is UCGAAGUACUCAGCGUAAAG.

The MTT (3-(4,5-dimethyl-thiazol-2-yl)-2,5-diphenyltetrazolium bromide, a yellow tetrazole) assay kit was purchased from Sigma-Aldrich (Saint-Quentin-Fallavier, France).

The cluster:siRNA complexes were prepared as follows: the clusters **A.Hyd** (20 mM in filtered RNase-free water) were vortexed for 5 s, ultrasonically mixed for 5 min, mixed with siRNA in order to reach the desired N/P, and incubated at room temperature for 20 min.

Fluorescence microscopy. MCF7-luc cells were seeded at a density of 50,000 cells per well and incubated for 24 h in a 8-well tissue culture chambers (Sarstedt, Germany) before treatment. The cells were incubated with **A8.Arg3**-Cy3-labeled siRNA complexes at a molar ratio of 25/1 (N/P=9) in OptiMEM (Invitrogen) for 4 h. These cells were then fixed with 500 μ L of cold 4% PFA for 30 min and washed twice with PBS. The nuclei were stained using a DAPI solution (Sigma-Aldrich, Saint Quentin-Fallavier, France). Images were taken with an inverted fluorescence microscope (Leica DMRB, Leica Microsystems GmbH, Germany) and analyzed using ImageJ software.

Cell luciferase assay. MCF7-luc cells were seeded at a density of 5000 cells per well in 96-well white opaque tissue culture plates in 150 μ L complete culture medium and incubated for 24 h. The cells were then washed with PBS and incubated with various cluster:siRNA complex formulations in OptiMEM at 37°C for 4 h. Thereafter, 50 μ L of 40% serum containing medium was added. Two days after transfection, expression of luciferase was assessed by addition into culture medium of luciferin (10⁻³ M, final concentration) purchased from Promega (France). Living cell luminescence was measured 10 min after by a multilabel plate reader (Wallac1420, PerkinElmer, USA)

for 5 s. Values are expressed as percentage of luciferase activity compared to non-treated wells (set as 100 %).

Cytotoxicity assay. The cytotoxicity of cluster:siRNA complexes was determined by the MTT assay. In brief, MCF7-luc cells were seeded at 5,000 cells/well in clear, flat-bottomed, 96-well plates (Costar) 24 h before treatment. After being washed, 150 μ l of OptiMEM that contained the cluster:siRNA complexes at different N/P ratios was added to the wells and incubated for 4 h. Thereafter, 50 μ l of 40% serum containing medium was added, and the cytotoxicity of the relevant reagents was determined by the MTT assay after 48 h. The absorbance at 540 nm was read on a plate reader (Multiskan FC, Thermo Fisher Scientific, France). The results obtained from triplicate wells were averaged and normalized to the value obtained from the non-treated cells.

Synthetic procedures.

Linear peptide A7. Similarly to the synthesis of cyclic peptide **A8**,¹⁸ the decapeptide was synthesized *via* SPPS strategy (0.25 mmol scale) using 2-Chlorotrityl Chloride resin and a Fmoc-Lys[Boc-Ser(*t*-Bu)]-OH²⁶ dipeptide. The resin was loaded with the first amino acid by reacting 3 g (4.8 mmol/Cl) of resin with 4.3 g (14.4 mmol, 3eq) of Fmoc-Gly-OH and 4.2 mL (24 mmol, 2M, 5 eq) of DIEA in 40 mL DMF/dichloromethane for 1.5 hour. The resin was then filtered, washed with MeOH, DMF (3x), CH₂Cl₂ (2x), diethyl ether (1x) and dried *in vacuo*. The loading was quantified by UV-Vis spectroscopy²⁷ as follows: 10 mg of resin were suspended in 1 mL of Piperidine/DMF (2/8) for 20 min and filtered. 100 μ l of the filtrate were dissolved in 10 mL of DMF and the absorbance was measured at 301 nm. The charge of the modified resin was determined to be 0.31 mmol/g, and it was then engaged in SPPS. The final acetylation was then carried out with 10 mL of a solution of acetic anhydride/CH₂Cl₂ (50/50) for 20 min (2x). The product was then cleaved and deprotected with a TFA/H₂O/TIS (95/2.5/2.5) solution (20 mL) for 2 hours. The filtrate was concentrated, precipitated by adding Et₂O, and centrifuged (10000 t/min for 10 min). The supernatant was removed and the crude material was freeze dried to give a white solid (326 mg, 71%). The oxidative cleavage was carried out by dissolving the crude material in 18.4 mL of H₂O and adding 403 mg (1.8 mmol, 10 eq) of sodium periodate. The desired product was then purified by semi-preparative HPLC using the following gradient of ACN/TFA 99.9/0.1 into H₂O: 0 to 25% in 25 min, then 25% to 100% in 10 min. 104 mg (47%) of a white solid were obtained (overall yield for the preparation of **A7**: 51%). HPLC: *t_R* 3.49 min; MALDI-ToF (HCCA): calcd for [C₅₄H₈₂N₁₄O₂₀+K]⁺ 1285.58, found 1285.52.

General procedure for the solid-phase synthesis of amino acid hydrazides. Preparation of the modified resin: DIEA (2.45 mL, 14.05 mmol) was added to a suspension of 2-Chlorotrityl Chloride resin (1.75 g, 2.81 mmol Cl/g) in NMP/DMSO (4/1) (9 mL). A solution of 9-Fluorenylmethyl carbamate (Fmoc-hydrazide, 2.14 g, 8.43 mmol) in DMSO (9 mL) was then added and the mixture was stirred for 2 hours. After filtration, capping was performed by mixing with MeOH for a few

minutes. The resin was then filtered, washed with DMSO (3x), CH₂Cl₂ (2x), isopropanol (1x), CH₂Cl₂ (2x) and Et₂O (3x), and dried *in vacuo*. The loading, calculated according to the procedure used in the synthesis of **A7**, was determined to be 0.39 mmol/g.

Peptide couplings procedure: The initial Fmoc deprotection was carried out as follows: the resin was suspended in a solution of Piperidine/NMP/DMSO (30/56/14) (2 mL). After 1h, it was filtered, washed with DMSO (3x), CH₂Cl₂ (2x), Isopropanol (1x), CH₂Cl₂ (2x), Et₂O (3x), and dried *in vacuo*. The resin (500 mg, 0.195 mmol) was suspended in a solution of NMP/DMSO (4/1) (500 μ l). The Fmoc-Amino acid-OH (0.351 mmol) was pre-activated by addition, in a solution of NMP/DMSO (4/1) (1 mL), of DIEA (98 μ l, 0.585 mmol) and HATU (133.5 mg, 0.351 mmol). After 30 min, the mixture of pre-activated amino acid was added to the resin. After 3 hours, the resin was filtered and this coupling procedure was repeated twice. The resin was then washed (DMSO (3x), CH₂Cl₂ (2x), Isopropanol (1x), CH₂Cl₂ (2x) and Et₂O (3x)) and dried. Capping was carried out by suspending the resin in a solution of acetic anhydride/CH₂Cl₂ (1/1) (2 mL) for 20 min (procedure repeated twice). The resin was then filtered, washed (DMSO (3x), CH₂Cl₂ (2x), Isopropanol (1x), CH₂Cl₂ (2x) and Et₂O (3x)) and dried *in vacuo*. Fmoc deprotection was carried out by suspending the resin in a solution of Piperidine/NMP/DMSO (30/56/14) (2 mL) for 1 hour. The resin was then filtered, washed and dried *in vacuo*.

Deprotection and cleavage procedure: The resin was suspended in a solution of TFA/TIS/H₂O (95/2.5/2.5) (5 mL) for 2 hours, then filtered and washed with CH₂Cl₂. The filtrate was partially concentrated *in vacuo*, and precipitated with Et₂O. After centrifugation and removal of the supernatant, the white solid was freeze dried.

2-aminoacetohydrazide (GlyHyd). GlyHyd was synthesized according general procedure (60.6 mg, quantitative). ¹H NMR (D₂O; 400 MHz) δ 3.88 (s, 2H, H₂N-CH₂); ¹³C NMR (D₂O; 100 MHz) δ 166.0, 163.1 (q, ²J(C,F)=35, 1C, F₃C-C=O), 117.8 (q, ¹J(C,F)=290, 1C, F₃C-), 39.2.

(S)-2-aminopropanehydrazide (AlaHyd). AlaHyd was synthesized according general procedure (21.2 mg, 67%). ¹H NMR (D₂O; 400 MHz) δ 4.19 (q, ²J=7.0, 1H, H₂N-CH), 1.57 (d, ²J=7.0, 3H, CH-CH₃); ¹³C NMR (D₂O; 100 MHz) δ 169.2, 163.1 (q, ²J(C,F)=35, 1C, F₃C-C=O), 117.8 (q, ¹J(C,F)=290, 1C, F₃C-), 47.9, 16.2; [α]_D²⁰: +8.1 (H₂O, c=1.0); HR-ESI-MS: calcd for [C₃H₉N₃O+H]⁺ 104.0824, found 104.0822.

(S)-3-amino-4-hydrazinyl-4-oxobutanoic acid (AspHyd). AspHyd was synthesized according general procedure (19.2 mg, 53%). ¹H NMR (D₂O; 400 MHz) δ 4.43 (m, 1H, CH-CH₂), 3.08 (m, 2H, CH-CH₂-CO); ¹³C NMR (D₂O; 100 MHz) δ 172.3, 167.3, 163.1 (q, ²J(C,F)=35, 1C, F₃C-C=O), 117.8 (q, ¹J(C,F)=290, 1C, F₃C-), 48.5, 34.6; [α]_D²⁰: +17.4 (H₂O, c=1.0); HR-ESI-MS: calcd for [C₄H₉N₃O₃+H]⁺ 148.0722, found 148.0720.

(S)-2-amino-3-(1H-imidazol-5-yl)propanehydrazide (HisHyd). HisHyd was synthesized according general procedure (26.1 mg, 68%). ¹H NMR (D₂O; 400 MHz) δ 8.72 (s, 1H, HN-CH=N), 7.46 (s, 1H, C=CH-N), 4.36 (t, ³J=7.0, 1H, CH-CH₂); ¹³C NMR (D₂O; 100 MHz) δ 166.6, 163.1 (q, ²J(C,F)=35, 1C, F₃C-C=O), 135.6, 125.4,

118.6, 117.8 (q, $^1J(\text{C},\text{F})=290$, 1C, $\text{F}_3\text{C}-$), 50.9, 25.8; $[\alpha]_{\text{D}}^{20}$: +18.0 (H_2O , $c=1.0$); HR-ESI-MS: calcd for $[\text{C}_6\text{H}_{11}\text{N}_5\text{O}+\text{H}]^+$ 170.1042, found 170.1041.

(S)-2,6-diaminohexanehydrazide (LysHyd). LysHyd was synthesized according general procedure (37.1 mg, 84%). ^1H NMR (D_2O ; 400 MHz) δ 4.08 (t, $^2J=7.0$, 1H, $\text{H}_2\text{N}-\text{CH}$), 2.99 (t, $^2J=7.6$, 2H, CH_2-NH_2), 1.94 (m, 2H, $\text{CH}_2-\text{CH}_2-\text{NH}_2$), 1.70 (m, 2H, $\text{CH}-\text{CH}_2$); ^{13}C NMR (D_2O ; 100 MHz) δ 168.2, 163.1 (q, $^2J(\text{C},\text{F})=35$, 1C, $\text{F}_3\text{C}-\text{C}=\text{O}$), 117.8 (q, $^1J(\text{C},\text{F})=290$, 1C, $\text{F}_3\text{C}-$), 51.8, 39.0, 30.1, 26.3, 21.2; $[\alpha]_{\text{D}}^{20}$: +16.8 (H_2O , $c=1.0$); HR-ESI-MS: calcd for $[\text{C}_6\text{H}_{16}\text{N}_4\text{O}+\text{H}]^+$ 161.1402, found 161.1402.

(S)-1-(4-amino-5-hydrazinyl-5-oxopentyl)guanidine (L-ArgHyd). L-ArgHyd was synthesized according general procedure (14.2 mg, 81%). ^1H NMR (D_2O ; 400 MHz) δ 4.10 (t, $^3J=6.7$, 1H, $\text{CH}-\text{CH}_2$), 3.24 (t, $^3J=6.8$, 2H, $\text{CH}_2-\text{CH}_2-\text{NH}$), 2.02-1.92 (m, 2H, $\text{CH}_2-\text{CH}_2-\text{NH}$), 1.72-1.64 (m, 2H, $\text{CH}-\text{CH}_2-\text{CH}_2$); ^{13}C NMR (D_2O ; 100 MHz) δ 168.2, 156.8, 51.6, 40.2, 27.7, 23.5; $[\alpha]_{\text{D}}^{20}$: +15.3 (H_2O , $c=1.0$); HR-ESI-MS: calcd for $[\text{C}_6\text{H}_{16}\text{N}_6\text{O}+\text{H}]^+$ 189.1464, found 189.1466.

(R)-1-(4-amino-5-hydrazinyl-5-oxopentyl)guanidine (D-ArgHyd). D-ArgHyd was synthesized according general procedure (67.6 mg, 75%). ^1H NMR (D_2O ; 400 MHz) δ 4.15 (t, $^3J=6.6$, 1H, $\text{CH}-\text{CH}_2$), 3.24 (t, $^3J=6.8$, 2H, CH_2-NH), 2.02-1.95 (m, 2H, $\text{CH}-\text{CH}_2$), 1.73-1.65 (m, 2H, $\text{CH}_2\text{CH}_2\text{NH}$); ^{13}C NMR (D_2O ; 100 MHz) δ 168.1, 163.1 (q, $^2J(\text{C},\text{F})=35$, 1C, $\text{F}_3\text{C}-\text{C}=\text{O}$), 156.9, 117.8 (q, $^1J(\text{C},\text{F})=290$, 1C, $\text{F}_3\text{C}-$), 51.6, 40.3, 27.8, 23.5; $[\alpha]_{\text{D}}^{20}$: -7.2 (H_2O , $c=1.0$); HR-ESI-MS: calcd for $[\text{C}_6\text{H}_{16}\text{N}_6\text{O}+\text{H}]^+$ 189.1464, found 189.1464.

(S)-2,6-diamino-N-((S)-6-amino-1-(((S)-6-amino-1-hydrazinyl-1-oxohexan-2-yl)amino)-1-oxohexan-2-yl)hexanamide (Lys₃Hyd). Lys₃Hyd was synthesized by SPPS on a 0.1 mmol scale using the modified Fmoc hydrazine resin that is manually prepared from the 2-Chlorotrityl Chloride resin as described above. After SPPS, the product was cleaved from the resin with a solution of TFA/ CH_2Cl_2 (1:99) (10 mL) (3 min, 3x). A solution of MeOH/Pyridine (8/2) (10 mL) was added to the filtrate and the solution was partially concentrated *in vacuo*. Et₂O was added to the crude product and a white precipitate appeared. The mixture was centrifuged, the supernatant was removed and the precipitate was freeze dried. The crude product was then purified on preparative HPLC using the following gradient of ACN/TFA 99.9/0.1 into H_2O : 20% to 40% in 20 min to obtain a white solid after freeze-drying. Final deprotection was carried out with TFA/ H_2O /TIS (95/2.5/2.5) (10 mL) for 2 hours. The deprotected product was partially concentrated *in vacuo*. Et₂O was then added and a white precipitate appeared. The mixture was centrifuged and the precipitate dried. Lys₃Hyd was freeze-dried and obtained as a white solid (49.3 mg, 52%). ^1H NMR (D_2O ; 400 MHz) δ 4.38-4.35 (m, 2H, $2\text{CH}-\text{CH}_2$), 4.07 (t, $^3J=6.0$, 1H, $\text{CH}-\text{CH}_2$), 3.05-3.04 (m, 6H, $3\text{CH}_2-\text{NH}_2$), 1.95-1.72 (m, 12H, $3\text{CH}-\text{CH}_2$, $3\text{CH}_2-\text{CH}_2-\text{NH}_2$), 1.55-1.45 (m, 6H, $3\text{CH}-\text{CH}_2-\text{CH}_2$); ^{13}C NMR (D_2O ; 100 MHz) δ 173.6, 171.8, 169.7, 163.1 (q, $^2J(\text{C},\text{F})=35$, 1C, $\text{F}_3\text{C}-\text{C}=\text{O}$), 117.8 (q, $^1J(\text{C},\text{F})=290$, 1C, $\text{F}_3\text{C}-$), 53.7, 52.8, 52.2, 39.2, 39.0, 30.6, 30.5, 30.3, 26.4, 26.3, 22.1, 22.0, 21.3; $[\alpha]_{\text{D}}^{20}$: -11.6 (H_2O , $c=1.0$); HR-ESI-MS: calcd for $[\text{C}_{18}\text{H}_{40}\text{N}_8\text{O}_3+\text{H}]^+$ 417.3302, found 417.3296.

(2S,2'S)-N,N'-((S)-6-hydrazinyl-6-oxohexane-1,5-diyl)bis(2,6-diaminohexanamide) (G₁-LysHyd). G₁-LysHyd was synthesized according to the general procedure for the solid-phase synthesis of amino acid hydrazides using Fmoc-L-Lys(Fmoc)-OH. The second coupling reaction was carried out with doubled quantities of reagents. Finally, the resin was suspended in a solution of TFA/TIS/ H_2O (95/2.5/2.5) (5 mL) for 2 hours, filtered and washed with CH_2Cl_2 . The filtrate was partially concentrated *in vacuo*, and precipitated with Et₂O. After centrifugation and removal of the supernatant, the white solid was freeze dried to afford G₁-LysHyd as a white solid (230.8 mg, 84%). ^1H NMR (MeOD; 400 MHz) δ 4.40 (bs, 1H, $\text{CH}-\text{CH}_2$), 3.96 (bs, 1H, $\text{CH}-\text{CH}_2$), 3.85 (bs, 1H, $\text{CH}-\text{CH}_2$), 3.25 (bs, 2H, CH_2-NH), 2.95 (bs, 4H, $2\text{CH}_2-\text{NH}$), 1.89-1.47 (m, 18H, $3\text{CH}-\text{CH}_2-\text{CH}_2$, $3\text{CH}_2-\text{CH}_2-\text{CH}_2$, $3\text{CH}_2-\text{NH}_2$); ^{13}C NMR (MeOD; 100 MHz) δ 170.2, 170.0, 54.3, 53.9, 53.6, 40.3, 40.3, 32.3, 32.1, 31.9, 29.8, 28.1, 28.0, 24.1, 22.9, 22.5; $[\alpha]_{\text{D}}^{20}$: +8.8 (H_2O , $c=1.0$); HR-ESI-MS: calcd for $[\text{C}_{18}\text{H}_{40}\text{N}_8\text{O}_3+\text{H}]^+$ 417.3302, found 417.3299.

(S)-2-amino-5-guanidino-N-((S)-5-guanidino-1-(((S)-5-guanidino-1-hydrazinyl-1-oxopentan-2-yl)amino)-1-oxopentan-2-yl)pentanamide (Arg₃Hyd). Arg₃Hyd was synthesized by SPPS on a 0.1 mmol scale using the modified Fmoc hydrazine resin that is manually prepared from the 2-Chlorotrityl Chloride resin as described above. After SPPS, the product was cleaved from the resin with a solution of TFA/ CH_2Cl_2 (1:99) (10 mL) (3 min, 3x). A solution of MeOH/Pyridine (8/2) (10 mL) was added to the filtrate and the solution was partially concentrated *in vacuo*. Et₂O was added to the crude product and a white precipitate appeared. The mixture was centrifuged, the supernatant was removed and the precipitate was freeze dried. The crude product was then purified on preparative HPLC using the following gradient of ACN/TFA 99.9/0.1 into H_2O : 20% to 70% in 45 min to afford a white solid after freeze-drying. Final deprotection was carried out with TFA/ H_2O /TIS (95/2.5/2.5) (10 mL) for 2 hours. The deprotected product was partially concentrated *in vacuo* and precipitated with Et₂O. The mixture was centrifuged and the precipitate dried. Arg₃Hyd was freeze-dried and obtained as a white solid (48.8 mg, 46%). ^1H NMR (D_2O ; 400 MHz) δ 4.43-4.37 (m, 2H, $2\text{CH}-\text{CH}_2$), 4.12 (t, $^3J=6.4$, 1H, $\text{CH}-\text{CH}_2$), 3.26-3.23 (m, 6H, $3\text{CH}_2-\text{NH}$), 1.99-1.80 (m, 6H, $3\text{CH}-\text{CH}_2$), 1.76-1.61 (m, 6H, $3\text{CH}-\text{CH}_2-\text{CH}_2$); ^{13}C NMR (D_2O ; 100 MHz) δ 173.6, 171.6, 169.7, 156.9, 53.7, 52.6, 52.0, 40.6, 40.4, 28.1, 28.0, 27.9, 24.4, 23.5; $[\alpha]_{\text{D}}^{20}$: -5.6 (H_2O , $c=1.0$); HR-ESI-MS: calcd for $[\text{C}_{18}\text{H}_{40}\text{N}_{14}\text{O}_3+\text{H}]^+$ 501.3486, found 501.3482.

General procedure for clusters synthesis through acylhydrazone ligation. 8 equivalents of hydrazide per scaffold were added from a 200 mM stock solution in water into a 1 mM solution of scaffold **A** in aqueous buffer (100 mM AcONa, pH 5.0) and the mixture was stirred overnight at room temperature. The resulting cluster was analyzed by HPLC and MALDI-ToF or HR-ESI mass spectrometry. Clusters **A8.Ac** and **A8.L-Arg** were prepared as previously described.¹⁸

A8.Gly MALDI-ToF (HCCA): calcd for $[\text{C}_{60}\text{H}_{98}\text{N}_{26}\text{O}_{18}+\text{Na}]^+$ 1493.76, found 1493.72. **A8.Gir** HPLC: t_{R} 6.83 min; MALDI-ToF (HCCA): calcd for $[\text{C}_{72}\text{H}_{127}\text{N}_{26}\text{O}_{18}+4\text{Cl}+\text{Na}]^+$ 1805.98, found 1805.86. **A8.Ala** MALDI-ToF (HCCA): calcd for

[C₆₄H₁₀₆N₂₆O₁₈+Na]⁺ 1549.82, found 1549.81. **A8.Asp** MALDI-ToF (HCCA): calcd for [C₆₈H₁₀₇N₂₆O₂₆+Na]⁺ 1726.78, found 1725.76. **A8.His** MALDI-ToF (HCCA): calcd for [C₇₆H₁₁₅N₃₄O₁₈+Na]⁺ 1814.91, found 1813.92. **A8.Lys** MALDI-ToF (HCCA): calcd for [C₇₆H₁₃₄N₃₀O₁₈+Na]⁺ 1778.05, found 1777.99. **A8.D-Arg** MALDI-ToF (HCCA): calcd for [C₇₆H₁₃₄N₃₈O₁₈+H]⁺ 1868.07, found 1868.05. **A8.Lys₃** HPLC: t_R 2.94 min; MALDI-ToF (HCCA): calcd for [C₁₂₄H₂₃₁N₄₆O₂₆+Na]⁺ 2803.82, found 2802.76. **A8.G₁-Lys** HPLC: t_R 4.66 min; MALDI-ToF (HCCA): calcd for [C₁₂₄H₂₃₁N₄₆O₂₆+Na]⁺ 2803.82, found 2802.79. **A8.Arg₃** HPLC: t_R 5.79 min; MALDI-ToF (HCCA): calcd for [C₁₂₄H₂₃₁N₇₀O₂₆+H]⁺ 3116.82, found 3116.86. **A1.Ac** HPLC: t_R 6.26 min; HR-ESI-MS: calcd for [C₉H₁₀N₂O+Na]⁺ 185.0871, found 185.0870. **A2.Ac** HPLC: t_R 7.40 min; HR-ESI-MS: calcd for [C₁₀H₁₀N₂O₂+Na]⁺ 213.0821, found 213.0819. **A3.Ac** HPLC: t_R 6.78 min; HR-ESI-MS: calcd for [C₁₂H₁₄N₄O₂+Na]⁺ 269.1195, found 269.1197. **A4.Ac** HPLC: t_R 6.92 min; HR-ESI-MS: calcd for [C₁₂H₁₄N₄O₂+Na]⁺ 269.1195, found 269.1197. **A5.Ac** HR-ESI-MS: calcd for [C₉H₁₆N₄O₂+Na]⁺ 235.1171, found 235.1169. **A6.Ac** HPLC: t_R 7.92 min; HR-ESI-MS: calcd for [C₁₅H₁₈N₆O₃+Na]⁺ 353.1519, found 353.1516. **A7.Ac** HPLC: t_R 7.99 min; MALDI-ToF (HCCA): calcd for [C₆₂H₉₈N₂₂O₂₀+Na]⁺ 1493.73, found 1493.70.

Acknowledgements

We thank the CNRS, the LabEx CheMISyst (ANR-10-LABX-05-01) and the ANR (ANR-11-PDOC-002-02) for funding. Automated peptide synthesis was carried out at the SynBio 3 platform – IBMM, Montpellier. We thank the ENSCM for the access to the fluorescence microplate reader. We thank Sarah Michel for her contribution to the peptide synthesis.

References

- 1 S. T. Crooke, *Annu. Rev. Med.*, 2004, **55**, 61-95; A. Demesmaeker, R. Haner, P. Martin and H. E. Moser, *Acc. Chem. Res.*, 1995, **28**, 366-374; E. Uhlmann and A. Peyman, *Chem. Rev.*, 1990, **90**, 543-584.
- 2 J. C. Burnett, J. J. Rossi and K. Tiemann, *Biotechnol. J.*, 2011, **6**, 1130-1146; J. W. Gaynor, B. J. Campbell and R. Cosstick, *Chem. Soc. Rev.*, 2010, **39**, 4169-4184; D. Castanotto and J. J. Rossi, *Nature*, 2009, **457**, 426-433.
- 3 M. A. Mintzer and E. E. Simanek, *Chem. Rev.*, 2009, **109**, 259-302; S. Lehrman, *Nature*, 1999, **401**, 517-518.
- 4 U. Lächelt and E. Wagner, *Chem. Rev.*, 2015, DOI: 10.1021/cr5006793.
- 5 S. K. Samal, M. Dash, S. V. Vlierberghe, D. L. Kaplan, E. Chiellini, C. v. Blitterswijk, L. Moroni and P. Dubruel, *Chem. Soc. Rev.*, 2012, **41**, 7147-7194; D. N. Nguyen, J. J. Green, J. M. Chan, R. Longer and D. G. Anderson, *Adv. Mater.*, 2009, **21**, 847-867; S. Y. Wong, J. M. Pelet and D. Putnam, *Prog. Polym. Sci.*, 2007, **32**, 799-837; T. Merdan, J. Kopecek and T. Kissel, *Adv. Drug Deliv. Rev.*, 2002, **54**, 715-758.
- 6 X. X. Liu, P. Rocchi and L. Peng, *New J. Chem.*, 2012, **36**, 256-263.
- 7 C. Fasting, C. A. Schalley, M. Weber, O. Seitz, S. Hecht, B. Koksich, J. Dervede, C. Graf, E. W. Knapp and R. Haag, *Angew. Chem. Int. Ed.*, 2012, **51**, 10472-10498; G. V. Oshovsky, D. N. Reinhoudt and W. Verboom, *Angew. Chem. Int. Ed.*, 2007, **46**, 2366-2393; L. L. Kiessling, J. E. Gestwicki and L. E. Strong, *Angew. Chem. Int. Ed.*, 2006, **45**, 2348-2368; J. D. Badjic, A. Nelson, S. J. Cantrill, W. B. Turnbull and J. F. Stoddart, *Acc. Chem. Res.*, 2005, **38**, 723-732; A. Mulder, J. Huskens and D. N. Reinhoudt, *Org. Biomol. Chem.*, 2004, **2**, 3409-3424; M. Mammen, S. K. Choi and G. M. Whitesides, *Angew. Chem. Int. Ed.*, 1998, **37**, 2755-2794.
- 8 S. M. Moghimi, P. Symonds, J. C. Murray, A. C. Hunter, G. Debska and A. Szewczyk, *Mol. Ther.*, 2005, **11**, 990-995.
- 9 For examples of disulfide-based bio-reducible polymers and dendrimers, see for instance: A. Barnard, P. Posocco, M. Fermiglia, A. Tschiche, M. Calderon, S. Prich and D. K. Smith, *Org. Biomol. Chem.*, 2014, **12**, 446-455; L. D. Feng, A. Xie, X. Y. Hu, Y. Y. Liu, J. F. Zhang, S. F. Li and W. Dong, *New J. Chem.*, 2014, **38**, 5207-5214; K. L. Kozielski, S. Y. Tzeng and J. J. Green, *Chem. Commun.*, 2013, **49**, 5319-5321; H. M. Liu, H. Wang, W. J. Yang and Y. Y. Cheng, *J. Am. Chem. Soc.*, 2012, **134**, 17680-17687; S. Son, R. Namgung, J. Kim, K. Singha and W. J. Kim, *Acc. Chem. Res.*, 2012, **45**, 1100-1112; Y. Wang, R. Zhang, N. Xu, F. S. Du, Y. L. Wang, Y. X. Tan, S. P. Ji, D. H. Liang and Z. C. Li, *Biomacromolecules*, 2011, **12**, 66-74; T. I. Kim, M. Lee and S. W. Kim, *Biomaterials*, 2010, **31**, 1798-1804; J. G. Hardy, C. S. Love, N. P. Gabrielson, D. W. Pack and D. K. Smith, *Org. Biomol. Chem.*, 2009, **7**, 789-793; Bauhuber, C. Hozsa, M. Breunig and A. Gopferich, *Adv. Mater.*, 2009, **21**, 3286-3306.
- 10 For examples of acid-sensitive materials, see for instance: C. Bouillon, D. Paolantoni, J. C. Rote, Y. Bessin, L. W. Peterson, P. Dumy and S. Ulrich, *Chem. Eur. J.*, 2014, **20**, 14705-14714; H. L. Cao, Y. X. Dong, A. Aied, T. Y. Zhao, X. Chen, W. X. Wang and A. Pandit, *Chem. Commun.*, 2014, **50**, 15565-15568; S. Binauld and M. H. Stenzel, *Chem. Commun.*, 2013, **49**, 2082-2102; B. J. Hong, A. J. Chipre and S. T. Nguyen, *J. Am. Chem. Soc.*, 2013, **135**, 17655-17658; S. Duan, W. Yuan, F. Wu and T. Jin, *Angew. Chem. Int. Ed.*, 2012, **51**, 7938-7941; L. N. Cui, J. L. Cohen, C. K. Chu, P. R. Wich, P. H. Kierstead and J. M. J. Frechet, *J. Am. Chem. Soc.*, 2012, **134**, 15840-15848; A. Barnard, P. Posocco, S. Prich, M. Calderon, R. Haag, M. E. Hwang, V. W. T. Shum, D. W. Pack and D. K. Smith, *J. Am. Chem. Soc.*, 2011, **133**, 20288-20300; J. A. Wolff and D. B. Rozema, *Mol Ther*, 2008, **16**, 8-15; D. B. Rozema, D. L. Lewis, D. H. Wakefield, S. C. Wong, J. J. Klein, P. L. Roesch, S. L. Bertin, T. W. Reppen, Q. Chu, A. V. Blokhin, J. E. Hagstrom and J. A. Wolff, *Proc. Natl. Acad. Sci. USA*, 2007, **104**, 12982-12987; A. Aissaoui, B. Martin, E. Kan, N. Oudrhiri, M. Hauchecorne, J. P. Vigneron, J.-M. Lehn and P. Lehn, *J. Med. Chem.*, 2004, **47**, 5210-5223.
- 11 P. L. Padnya, E. A. Andreyko, O. A. Mostovaya, I. K. Rizvanov and I. I. Stoikov, *Org. Biomol. Chem.*, 2015, **13**, 5894-5904; V. Bagnacani, V. Franceschi, L. Fantuzzi, A. Casnati, G. Donofrio, F. Sansone and R. Ungaro, *Bioconjugate Chem.*, 2012, **23**, 993-1002; F. Sansone, L. Baldini, A. Casnati and R. Ungaro, *New J. Chem.*, 2010, **34**, 2715-2728; V. Bagnacani, F. Sansone,

- G. Donofrio, L. Baldini, A. Casnati and R. Ungaro, *Org. Lett.*, 2008, **10**, 3953-3956; F. Sansone, M. Dudic, G. Donofrio, C. Rivetti, L. Baldini, A. Casnati, S. Cellai and R. Ungaro, *J. Am. Chem. Soc.*, 2006, **128**, 14528-14536.
- 12 V. Bagnacani, V. Franceschi, M. Bassi, M. Lomazzi, G. Donofrio, F. Sansone, A. Casnati and R. Ungaro, *Nat. Commun.*, 2013, **4**, 1721.
- 13 D. Sigwalt, M. Holler, J. Iehl, J. F. Nierengarten, M. Nothisen, E. Morin and J. S. Remy, *Chem. Commun.*, 2011, **47**, 4640-4642.
- 14 Y. C. Chang, K. Yang, P. Wei, S. S. Huang, Y. X. Pei, W. Zhao and Z. C. Pei, *Angew. Chem. Int. Ed.*, 2014, **53**, 13126-13130; I. Nierengarten, M. Nothisen, D. Sigwalt, T. Biellmann, M. Holler, J. S. Remy and J. F. Nierengarten, *Chem. Eur. J.*, 2013, **19**, 17552-17558.
- 15 V. Villari, A. Mazzaglia, R. Darcy, C. M. O'Driscoll and N. Micali, *Biomacromolecules*, 2013, **14**, 811-817; A. Martinez, C. Bienvenu, J. L. J. Blanco, P. Vierling, C. O. Mellett, J. M. G. Fernandez and C. Di Giorgio, *J. Org. Chem.*, 2013, **78**, 8143-8148; C. Bienvenu, A. Martinez, J. L. J. Blanco, C. Di Giorgio, P. Vierling, C. O. Mellett, J. Defaye and J. M. G. Fernandez, *Org. Biomol. Chem.*, 2012, **10**, 5570-5581; A. Mendez-Ardoy, N. Guilloteau, C. Di Giorgio, P. Vierling, F. Santoyo-Gonzalez, C. O. Mellet and J. M. G. Fernandez, *J. Org. Chem.*, 2011, **76**, 5882-5894; A. Diaz-Moscoso, L. Le Gourrierc, M. Gomez-Garcia, J. M. Benito, P. Balbuena, F. Ortega-Caballero, N. Guilloteau, C. Di Giorgio, P. Vierling, J. Defaye, C. O. Mellet and J. M. G. Fernandez, *Chem. Eur. J.*, 2009, **15**, 12871-12888; A. Diaz-Moscoso, P. Balbuena, M. Gomez-Garcia, C. O. Mellet, J. M. Benito, L. Le Gourrierc, C. Di Giorgio, P. Vierling, A. Mazzaglia, N. Micali, J. Defaye and J. M. G. Fernandez, *Chem. Commun.*, 2008, 2001-2003; F. Ortega-Caballero, C. O. Mellet, L. Le Gourrierc, N. Guilloteau, C. Di Giorgio, P. Vierling, J. Defaye and J. M. G. Fernandez, *Org. Lett.*, 2008, **10**, 5143-5146.
- 16 X. Zhang, Z. Zhang, X. Xu, Y. Li, Y. Li, Y. Jian and Z. Gu, *Angew. Chem. Int. Ed.*, 2015, **54**, 4289-4294; X. X. Liu, J. H. Zhou, T. Z. Yu, C. Chen, Q. Cheng, K. Sengupta, Y. Y. Huang, H. T. Li, C. Liu, Y. Wang, P. Posocco, M. H. Wang, Q. Cui, S. Giorgio, M. Fermeglia, F. Q. Qu, S. Pricl, Y. H. Shi, Z. C. Liang, P. Rocchi, J. J. Rossi and L. Peng, *Angew. Chem. Int. Ed.*, 2014, **53**, 11822-11827; S. P. Jones, N. P. Gabrielson, C. H. Wong, H. F. Chow, D. W. Pack, P. Posocco, M. Fermeglia, S. Pricl and D. K. Smith, *Molecular Pharmaceutics*, 2011, **8**, 416-429; D. J. Welsh, S. P. Jones and D. K. Smith, *Angew. Chem. Int. Ed.*, 2009, **48**, 4047-4051; S. P. Jones, N. P. Gabrielson, D. W. Pack and D. K. Smith, *Chem. Commun.*, 2008, 4700-4702; M. A. Kostianen, J. G. Hardy and D. K. Smith, *Angew. Chem. Int. Ed.*, 2005, **44**, 2556-2559.
- 17 G. M. Pavan, M. A. Kostianen and A. Danani, *Rsc Adv*, 2011, **1**, 1677-1681; P. Posocco, S. Pricl, S. Jones, A. Barnard and D. K. Smith, *Chem Sci*, 2010, **1**, 393-404; G. M. Pavan, A. Danani, S. Pricl and D. K. Smith, *J. Am. Chem. Soc.*, 2009, **131**, 9686-9694.
- 18 E. Bartolami, Y. Bessin, V. Gervais, P. Dumy and S. Ulrich, *Angew. Chem. Int. Ed.*, 2015, DOI: 10.1002/anie.201504047.
- 19 C. Gehin, J. Montenegro, E.-K. Bang, A. Cajaraville, S. Takayama, H. Hirose, S. Futaki, S. Matile and H. Riezman, *J. Am. Chem. Soc.*, 2013, **135**, 9295-9298; J. Montenegro, E. K. Bang, N. Sakai and S. Matile, *Chem. Eur. J.*, 2012, **18**, 10436-10443; J. Montenegro, A. Fin and S. Matile, *Org. Biomol. Chem.*, 2011, **9**, 2641-2647; J. Montenegro, P. Bonvin, T. Takeuchi and S. Matile, *Chem. Eur. J.*, 2010, **16**, 14159-14166.
- 20 Y. C. Huang, C. C. Chen, S. J. Li, S. Gao, J. Shi and Y. M. Li, *Tetrahedron*, 2014, **70**, 2951-2955.
- 21 D. L. Boger, B. E. Fink, S. R. Brunette, W. C. Tse and M. P. Hedrick, *J. Am. Chem. Soc.*, 2001, **123**, 5878-5891.
- 22 K. E. Hauschild, J. S. Stover, D. L. Boger and A. Z. Ansari, *Bioorg. Med. Chem. Lett.*, 2009, **19**, 3779-3782.
- 23 C. D. Carlson, C. L. Warren, K. E. Hauschild, M. S. Ozers, N. Qadir, D. Bhimsaria, Y. Lee, F. Cerrina and A. Z. Ansari, *Proc. Natl. Acad. Sci. USA*, 2010, **107**, 4544-4549; W. C. Tse and D. L. Boger, *Acc. Chem. Res.*, 2004, **37**, 61-69.
- 24 G. Gasparini, E.-K. Bang, J. Montenegro and S. Matile, *Chem. Commun.*, 2015, **51**, 10389-10402; A. Mann, G. Thakur, V. Shukla, A. K. Singh, R. Khanduri, R. Naik, Y. Jiang, N. Kalra, B. S. Dwarakanath, U. Langel and M. Ganguli, *Mol. Pharmaceutics*, 2011, **8**, 1729-1741.
- 25 H. Y. Kuchelmeister, S. Karczewski, A. Gutschmidt, S. Knauer and C. Schmuck, *Angew. Chem. Int. Ed.*, 2013, **52**, 14016-14020.
- 26 S. Foillard, M. O. Rasmussen, J. Razkin, D. Boturyn and P. Dumy, *J. Org. Chem.*, 2008, **73**, 983-991.
- 27 C. Kay, O. E. Lorthioir, N. J. Parr, M. Congreve, S. C. McKeown, J. J. Scicinski and S. V. Ley, *Biotechnol Bioeng*, 2000, **71**, 110-118.